

INGRAM: Inductive Knowledge Graph Embedding via Relation Graphs

Jaejun Lee¹ Chanyoung Chung¹ Joyce Jiyoung Whang¹

Abstract

Inductive knowledge graph completion has been considered as the task of predicting missing triplets between new entities that are not observed during training. While most inductive knowledge graph completion methods assume that all entities can be new, they do not allow new relations to appear at inference time. This restriction prohibits the existing methods from appropriately handling real-world knowledge graphs where new entities accompany new relations. In this paper, we propose an Inductive knowledge GRAPH eMbedding method, INGRAM, that can generate embeddings of new relations as well as new entities at inference time. Given a knowledge graph, we define a relation graph as a weighted graph consisting of relations and the affinity weights between them. Based on the relation graph and the original knowledge graph, INGRAM learns how to aggregate neighboring embeddings to generate relation and entity embeddings using an attention mechanism. Experimental results show that INGRAM outperforms 14 different state-of-the-art methods on varied inductive learning scenarios.

1. Introduction

Knowledge graphs represent known facts as a set of triplets, each of which is composed of a head entity, a relation, and a tail entity (Ji et al., 2022). Among various approaches to predicting missing triplets in knowledge graphs, embedding-based methods are known to be effective, where entities and relations are converted into low-dimensional embedding vectors (Nathani et al., 2019). Classical knowledge graph embedding models (Liu et al., 2017; Sun et al., 2019) assume a transductive learning. That is, it is assumed that all entities and relations are observed during training. Transductive knowledge graph embedding methods predict a missing

¹School of Computing, KAIST, Daejeon, South Korea. Correspondence to: Joyce Jiyoung Whang <jjwhang@kaist.ac.kr>.

Proceedings of the 40th International Conference on Machine Learning, Honolulu, Hawaii, USA. PMLR 202, 2023. Copyright 2023 by the author(s).

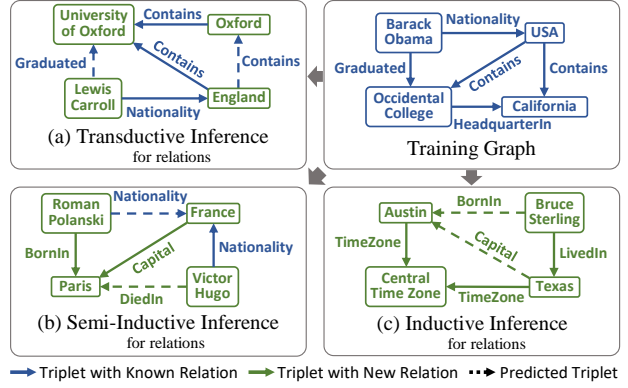


Figure 1: For relations, (a) is a transductive inference, (b) is a semi-inductive inference, and (c) is an inductive inference.

triplet by identifying a plausible combination of the observed entities and relations (Wang et al., 2017).

In recent years, inductive knowledge graph completion has been studied to predict missing triplets between new entities that are not observed at training time (Teru et al., 2020). If an entity or a relation is observed during training, we call them *known* and *new* otherwise; they are sometimes referred to as *seen* and *unseen* (Xu et al., 2022). To handle new entities, some methods focus on learning entity-independent relational patterns by logical rule mining (Sadeghian et al., 2019), while others exploit Graph Neural Networks (GNNs) (Yan et al., 2022). However, most existing methods assume that only entities can be new, and all relations should be observed during training. Thus, they perform inductive inference for entities but *transductive* inference for *relations* as shown in Figure 1(a).

In this paper, we consider more realistic inductive learning scenarios: (i) the relations at inference time consist of a mixture of known and new relations (*semi-inductive* inference for *relations*), or (ii) the relations are all new due to an entirely new set of entities (*inductive* inference for *relations*). Figure 1(b) and Figure 1(c) show these scenarios. We propose INGRAM, an INductive knowledge GRAPH eMbedding method that can generate embedding vectors for new relations and entities only appearing at inference time. Figure 2 shows an overview of INGRAM when all relations and entities are new. A key idea is to define a relation graph

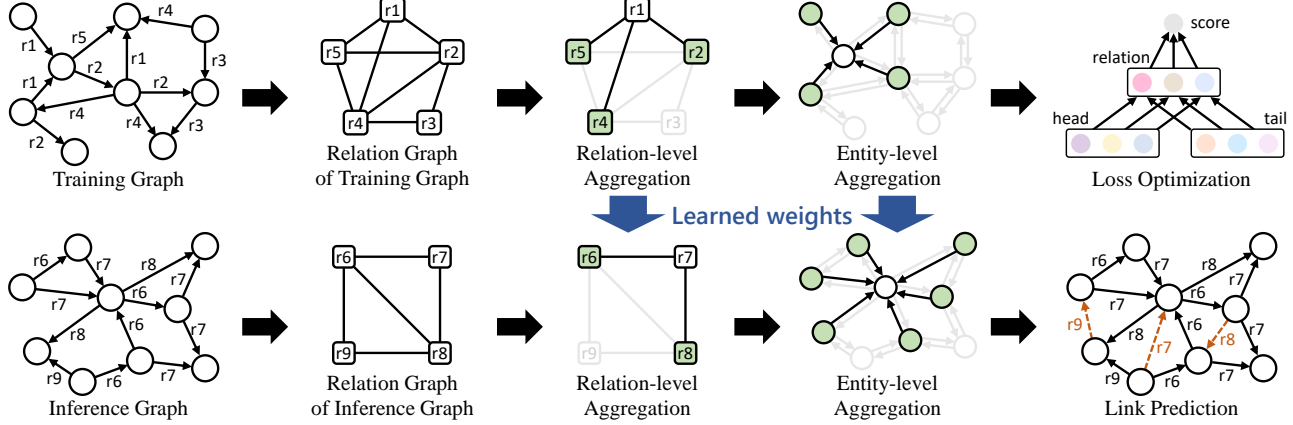


Figure 2: Overview of INGRAM. Given a knowledge graph, a relation graph is created to define the neighboring relations of each relation. Based on the relation graph and the original knowledge graph, relation and entity embedding vectors are computed by aggregating their neighbors’ embeddings. During training, INGRAM learns how to aggregate the neighbors’ embeddings by maximizing the scores of training triplets. At inference time, INGRAM generates embeddings of new relations and entities by aggregating neighbors’ embeddings based on the new relation graph computed from a given inference knowledge graph and the attention weights learned during training.

where a node corresponds to a relation, and an edge weight indicates the affinity between relations. Once the relation graph is defined, we can designate *neighboring* relations for each relation. Given the relation graph and the original knowledge graph, the relation and entity embedding vectors are computed by attention-based aggregations of their neighbors’ embeddings. The aggregation process is optimized to maximize the plausibility scores of triplets in a training knowledge graph. What INGRAM learns during training is *how to aggregate neighboring embeddings* to generate the relation and entity embeddings. At inference time, INGRAM generates embeddings of new relations and entities by aggregating neighbors’ embeddings based on the new relation graph computed from a given inference knowledge graph and the attention weights learned during training.

To the best of our knowledge, INGRAM is the first method that introduces the relation-level aggregation that allows the model to be generalizable to new relations. Due to the fully inductive capability of INGRAM, we can generate embeddings by training INGRAM on a tractable, partially observed set and simply applying it to an entirely new set without retraining. Different from some inductive methods that rely on large language models (Zha et al., 2022), INGRAM makes inferences solely based on the structure of a given knowledge graph. Experimental results show that INGRAM significantly outperforms 14 different knowledge graph completion methods in inductive link prediction on 12 datasets with varied ratios of new relations and entities. The performance gap between INGRAM and the best baseline method is substantial, especially when the ratio of new relations is high, which is a more challenging scenario.¹

2. Related Work

Rule Mining and Subgraph Reasoning. For inductive knowledge graph completion, (Yang et al., 2017) and (Sadeghian et al., 2019) have proposed learning first-order logical rules, while (Wang et al., 2021), (Zhu et al., 2021) and (Zhang & Yao, 2022) have considered relational context or paths. GraIL (Teru et al., 2020) has proposed a subgraph-based reasoning framework that extracts subgraphs and scores them using a GNN. Some follow-up works of GraIL include (Mai et al., 2021), (Xu et al., 2022), and (Lin et al., 2022). (Yan et al., 2022) has focused on cycle-based rule learning while (Liu et al., 2021) has proposed GNN-based encoding capturing logical rules. Different from our method, all these methods assume only entities can be new, and relations should be known in advance. (Jin et al., 2022) has recently proposed GraphANGEL handling new relations, but it assumes all entities are known.

Differences between RMPI and INGRAM. RMPI (Geng et al., 2023) has concurrently studied the problem of handling new relations, although how RMPI and INGRAM solve the problem is quite different. While RMPI extracts a local subgraph for every candidate entity to score the corresponding triplet, INGRAM directly utilizes the whole structure of a given knowledge graph. Also, RMPI uses an unweighted relation view per every individual triplet, whereas INGRAM defines one global relation graph where weights are important. Due to these fundamental differences, INGRAM is much more scalable and effective than RMPI. For example, INGRAM took 15 minutes and RMPI took 52 hours to process NL-100 dataset while INGRAM achieves much better link prediction performance than RMPI. Details will

¹<https://github.com/bdi-lab/InGram>

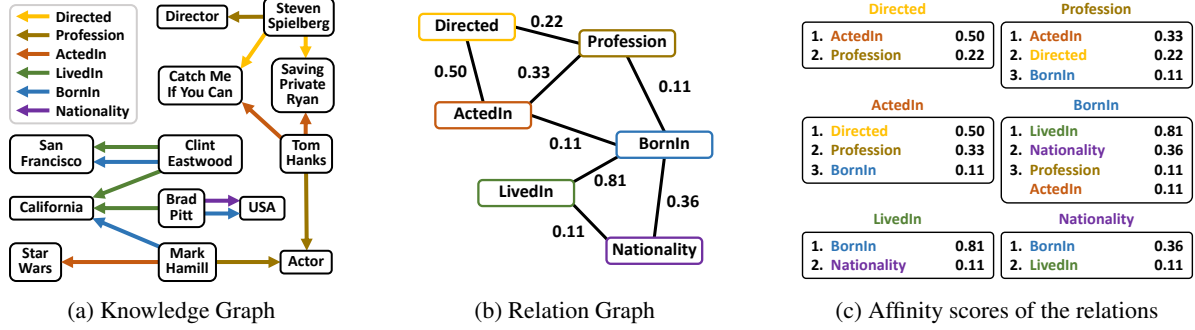


Figure 3: Given a knowledge graph, we define a relation graph as a weighted graph where each node indicates a relation, and each edge weight indicates the affinity between two relations. Self-loops in the relation graph are omitted for brevity.

be discussed in Section 6. Furthermore, RMPI is designed only for knowledge graph completion and does not compute embedding vectors, while INGRAM returns a set of embedding vectors for entities and relations that can be also utilized in many other downstream tasks.

Reasoning on Evolving Graphs. Some methods have focused on modeling emerging entities (Hamaguchi et al., 2017; Wang et al., 2022). For example, (Wang et al., 2019) has considered rule and network-based attention weights, and (Dai et al., 2021) has extended RotatE (Sun et al., 2019). All these methods assume that a triplet should be composed of one known entity and one new entity. (Cui et al., 2022) has proposed a GCN-based (Kipf & Welling, 2017) method to more flexibly handle emerging entities. Compared to these methods, we tackle a more challenging problem where all entities are new instead of only some portions being new.

Textual Descriptions and Language Models. (Daza et al., 2021), (Ali et al., 2021) and (Gesese et al., 2022) have used pre-trained vectors by BERT (Devlin et al., 2019) using textual descriptions. Some methods have utilized language models to handle new entities (Markowitz et al., 2022). For example, (Zha et al., 2022) has leveraged a pre-trained language model and fine-tuned it. All these methods employ a rich language model or require text descriptions that might not always be available. On the other hand, INGRAM only utilizes the structure of a given knowledge graph.

3. Problem Definition and Setting

In inductive knowledge graph embedding, we are given two graphs: a training graph $\widetilde{G}_{\text{tr}}$ and an inference graph $\widetilde{G}_{\text{inf}}$. A training graph is defined by $\widetilde{G}_{\text{tr}} = (\mathcal{V}_{\text{tr}}, \mathcal{R}_{\text{tr}}, \mathcal{E}_{\text{tr}})$ where \mathcal{V}_{tr} is a set of entities, \mathcal{R}_{tr} is a set of relations, and \mathcal{E}_{tr} is a set of triplets in $\widetilde{G}_{\text{tr}}$. We divide \mathcal{E}_{tr} into two disjoint sets such as $\mathcal{E}_{\text{tr}} := \mathcal{F}_{\text{tr}} \cup \mathcal{T}_{\text{tr}}$ where \mathcal{F}_{tr} is a set of known facts and \mathcal{T}_{tr} is a set of triplets a model is optimized to predict. An inference graph is defined by $\widetilde{G}_{\text{inf}} = (\mathcal{V}_{\text{inf}}, \mathcal{R}_{\text{inf}}, \mathcal{E}_{\text{inf}})$.

where \mathcal{V}_{inf} is a set of entities, \mathcal{R}_{inf} is a set of relations, and \mathcal{E}_{inf} is a set of triplets in $\widetilde{G}_{\text{inf}}$. We partition \mathcal{E}_{inf} into three pairwise *disjoint* sets, such that $\mathcal{E}_{\text{inf}} := \mathcal{F}_{\text{inf}} \cup \mathcal{T}_{\text{val}} \cup \mathcal{T}_{\text{test}}$ with a ratio of 3:1:1. \mathcal{F}_{inf} is a set of observed facts where it contains all entities and relations included in $\widetilde{G}_{\text{inf}}$, \mathcal{T}_{val} is a set of triplets for validation, and $\mathcal{T}_{\text{test}}$ is a set of test triplets. The fact sets \mathcal{F}_{tr} and \mathcal{F}_{inf} are also defined in (Zhang & Yao, 2022; Ali et al., 2021). Note that $\mathcal{V}_{\text{tr}} \cap \mathcal{V}_{\text{inf}} = \emptyset$ by following a conventional inductive learning setting (Teru et al., 2020). Most existing methods assume $\mathcal{R}_{\text{inf}} \subseteq \mathcal{R}_{\text{tr}}$ due to the constraint that relations cannot be new at inference time (Zhang & Yao, 2022). On the other hand, in our problem setting, \mathcal{R}_{inf} is not necessarily a subset of \mathcal{R}_{tr} since new relations are allowed to appear.

At training time, we use $G_{\text{tr}} := (\mathcal{V}_{\text{tr}}, \mathcal{R}_{\text{tr}}, \mathcal{F}_{\text{tr}})$ and a model is trained to predict \mathcal{T}_{tr} . When tuning the hyperparameters of a model, we use $G_{\text{inf}} := (\mathcal{V}_{\text{inf}}, \mathcal{R}_{\text{inf}}, \mathcal{F}_{\text{inf}})$ to compute the embeddings; we check the model’s performance on \mathcal{T}_{val} . At inference time, we evaluate the model’s performance using $\mathcal{T}_{\text{test}}$. The way we use \mathcal{F}_{inf} , \mathcal{T}_{val} and $\mathcal{T}_{\text{test}}$ is identical to (Ali et al., 2021; Galkin et al., 2022). For brevity, we do not explicitly mention G_{tr} or G_{inf} in the following sections; those should be distinguished in context.

4. Defining Relation Graphs

Let us represent a knowledge graph as $G = (\mathcal{V}, \mathcal{R}, \mathcal{F})$ where \mathcal{V} is a set of entities, \mathcal{R} is a set of relations, and \mathcal{F} is a set of triplets, i.e., $\mathcal{F} = \{(v_i, r_k, v_j) | v_i \in \mathcal{V}, r_k \in \mathcal{R}, v_j \in \mathcal{V}\}$. For every $(v_i, r_k, v_j) \in \mathcal{F}$, we add a reverse relation r_k^{-1} to \mathcal{R} and add a reverse triplet (v_j, r_k^{-1}, v_i) to \mathcal{F} (Schlichtkrull et al., 2018). Assume that $|\mathcal{V}| = n$ and $|\mathcal{R}| = m$.

Given a knowledge graph, we define a relation graph as a weighted graph where each node corresponds to a relation, and each edge weight indicates the affinity between two relations. Figure 3 shows an example where we omit the reverse relations and self-loops in the relation graph for simplicity.

Briefly speaking, we measure the affinity between two relations by considering how many entities are shared between them and how frequently they share the same entity.

To represent which relations are associated with which entities, we create two matrices $\mathbf{E}_h \in \mathbb{R}^{n \times m}$ and $\mathbf{E}_t \in \mathbb{R}^{n \times m}$ where the subscripts h and t indicate head and tail, respectively. Let $\mathbf{E}_h[i, j]$ denote the i -th row and the j -th column element of \mathbf{E}_h , where $\mathbf{E}_h[i, j]$ is the frequency of v_i appearing as a head entity of relation r_j . Similarly, $\mathbf{E}_t[i, j]$ is the frequency of v_i appearing as a tail entity of relation r_j . While some entities are frequently involved in relations, some entities are rarely involved in relations. To take this into account, we define the degree of an entity to be the sum of its frequencies. Formally, we define $\mathbf{A}_h := \mathbf{E}_h^T \mathbf{D}_h^{-2} \mathbf{E}_h$ where $\mathbf{D}_h \in \mathbb{R}^{n \times n}$ is the degree diagonal matrix of entities for head, i.e., $\mathbf{D}_h[i, i] := \sum_j \mathbf{E}_h[i, j]$. Similarly, we define $\mathbf{A}_t := \mathbf{E}_t^T \mathbf{D}_t^{-2} \mathbf{E}_t$ where $\mathbf{D}_t \in \mathbb{R}^{n \times n}$ is the degree diagonal matrix of entities for tail. The degree normalization terms allow the sum of the affinity weights introduced by each entity in \mathbf{A}_h and \mathbf{A}_t to be normalized to one.

Finally, we define the adjacency matrix of the relation graph to be $\mathbf{A} := \mathbf{A}_h + \mathbf{A}_t$ where $\mathbf{A} \in \mathbb{R}^{m \times m}$ and each element $a_{ij} \in \mathbf{A}$ indicates the affinity between the relations r_i and r_j . In Figure 3, we see that the relation graph identifies semantically close relations even though we use only the structure of a knowledge graph. However, there is a chance that we miss some semantically similar relation pairs in the relation graph if they do not share an entity in the knowledge graph. Note that the goal of the relation graph is not to identify the perfect set of similar relations but to define a relation's reasonable neighborhood whose representation vectors can be used to create the embedding of the target relation, which will be discussed in Section 5.1.

5. INGRAM: Inductive Knowledge Graph Embedding Model

We present INGRAM that consists of relation-level aggregation, entity-level aggregation, and modeling of relation-entity interactions.

5.1. Updating Relation Representation Vectors via Relation-Graph-Based Aggregation

Suppose we have an initial feature vector for a relation r_i , denoted by $\mathbf{x}_i \in \mathbb{R}^d$ ($i = 1, \dots, m$), where d is the dimension of a relation vector. We initialize \mathbf{x}_i using Glorot initialization (Glorot & Bengio, 2010). Let $\mathbf{z}_i^{(l)} \in \mathbb{R}^{d'}$ denote a hidden representation of r_i where d' is the hidden dimension, the superscript (l) indicates the l -th layer with $l = 0, \dots, L - 1$, and L is the number of layers for relations. We compute $\mathbf{z}_i^{(0)} = \mathbf{H} \mathbf{x}_i$ where $\mathbf{H} \in \mathbb{R}^{d' \times d}$ is a trainable

matrix that projects the initial feature vector to a hidden representation vector. All vectors are assumed to be column vectors unless specified.

Since we define the relation graph \mathbf{A} in Section 4, we can designate the neighboring relations of each relation using \mathbf{A} . We update each relation's representation by aggregating its own and neighbors' representation vectors. Specifically, we define the forward propagation as follows:

$$\mathbf{z}_i^{(l+1)} = \sigma \left(\sum_{r_j \in \mathcal{N}_i} \alpha_{ij}^{(l)} \mathbf{W}^{(l)} \mathbf{z}_j^{(l)} \right) \quad (1)$$

where $\sigma(\cdot)$ is an element-wise activation function such as LeakyReLU (Maas et al., 2013), $\mathbf{z}_j^{(l)}$ is a relation representation vector of r_j , $\mathbf{W}^{(l)} \in \mathbb{R}^{d' \times d'}$ is a weight matrix, \mathcal{N}_i is the set of neighbors of r_i on the relation graph \mathbf{A} , and the attention value $\alpha_{ij}^{(l)}$ is defined by²

$$\alpha_{ij}^{(l)} = \frac{\exp \left(\mathbf{y}^{(l)} \sigma \left(\mathbf{P}^{(l)} [\mathbf{z}_i^{(l)} \| \mathbf{z}_j^{(l)}] \right) + c_{s(i,j)}^{(l)} \right)}{\sum_{r_{j'} \in \mathcal{N}_i} \exp \left(\mathbf{y}^{(l)} \sigma \left(\mathbf{P}^{(l)} [\mathbf{z}_i^{(l)} \| \mathbf{z}_{j'}^{(l)}] \right) + c_{s(i,j')}^{(l)} \right)} \quad (2)$$

where $\|$ denotes concatenating vectors vertically, $\mathbf{P}^{(l)} \in \mathbb{R}^{d' \times 2d'}$ is a weight matrix, and $\mathbf{y}^{(l)} \in \mathbb{R}^{1 \times d'}$ is a row weight vector. We apply $\mathbf{y}^{(l)}$ after $\sigma(\cdot)$ to resolve the static attention issue of (Veličković et al., 2018) by following (Brody et al., 2022). In our implementation, we use the residual connection (He et al., 2016) and the multi-head attention mechanism with K heads (Vaswani et al., 2017). In (2), $c_{s(i,j)}^{(l)}$ is a learnable parameter indexed by $s(i, j)$ which is defined by

$$s(i, j) = \left\lceil \frac{\text{rank}(a_{ij}) \times B}{\text{nnz}(\mathbf{A})} \right\rceil \quad (3)$$

where a_{ij} indicates the value corresponding to the i -th row and the j -th column in \mathbf{A} , $\text{rank}(a_{ij})$ is the ranking of a_{ij} when the non-zero elements in \mathbf{A} are sorted in descending order, $\text{nnz}(\mathbf{A})$ is the number of non-zero elements in \mathbf{A} , and B is a hyperparameter indicating the number of bins. We divide the relation pairs into B different bins according to their affinity scores, i.e., the a_{ij} values. Each relation pair has an index value of $1 \leq s(i, j) \leq B$ and we have the learnable parameters $c_1^{(l)}, \dots, c_B^{(l)}$.

In (1) and (2), we update the relation representation vectors by using the attention mechanism, where we consider the relative importance of each neighboring relation and the affinity between the relations. While the former term is computed based on the local structure of the target relation, the latter term, $c_{s(i,j)}^{(l)}$, reflects a global level of affinity

²Note that \mathcal{N}_i includes r_i itself because \mathbf{A} contains self-loops.

because we divide the affinity scores into B different levels globally. When representing a relation's representation vector, it would be beneficial to take the vectors of similar relations to the target relation. Thus, $c_{s(i,j)}^{(l)}$ is expected to have a high value for a small $s(i,j)$ because the relation pairs belonging to a small $s(i,j)$ indicate those having high affinity values. We empirically observed that $c_{s(i,j)}^{(l)}$ values are learned as expected (details in Section 6.5). The way we incorporate the affinity into the attention mechanism is inspired by Graphomer (Ying et al., 2021) even though it is not designed for inductive knowledge graph embedding.

By updating $\mathbf{z}_i^{(l)}$ for $l = 0, \dots, L-1$ using (1), we have the final-level relation representation vectors $\mathbf{z}_i^{(L)}$ for $i = 1, \dots, m$ which are utilized to update entity representation vectors.

5.2. Entity Representation by Entity-level Aggregation

Suppose we have an initial feature vector for an entity v_i , denoted by $\hat{\mathbf{x}}_i \in \mathbb{R}^{\hat{d}}$ ($i = 1, \dots, n$), where \hat{d} is the dimension of an entity vector. We initialize $\hat{\mathbf{x}}_i$ using Glorot initialization. Let $\mathbf{h}_i^{(l)} \in \mathbb{R}^{\hat{d}^l}$ denote a hidden representation of v_i where \hat{d}^l is the hidden dimension, the superscript (l) indicates the l -th layer with $l = 0, \dots, \hat{L}-1$, and \hat{L} is the number of layers for entities. We compute $\mathbf{h}_i^{(0)} = \hat{\mathbf{H}}\hat{\mathbf{x}}_i$ where $\hat{\mathbf{H}} \in \mathbb{R}^{\hat{d}^0 \times \hat{d}}$ is trainable.

We update a representation vector of v_i by aggregating the representation vectors of its neighbors, its own vector, and the representation vectors of the relations adjacent to v_i . When we refer to the relation representation vectors here, we always use the final-level relation representation vectors $\mathbf{z}_k^{(L)}$ for $k = 1, \dots, m$ acquired in Section 5.1.

We define the neighbors of $v_i \in \mathcal{V}$ to be $\mathcal{N}_i = \{v_j | (v_j, r_k, v_i) \in \mathcal{F}, v_j \in \mathcal{V}, r_k \in \mathcal{R}\}$. To compute the attention weight for the self-loop of v_i , we consider the mean vector of the representation vectors of the relations adjacent to v_i :

$$\bar{\mathbf{z}}_i^{(L)} = \sum_{v_j \in \mathcal{N}_i} \sum_{r_k \in \mathcal{R}_{ji}} \frac{\mathbf{z}_k^{(L)}}{\sum_{v_j \in \mathcal{N}_i} |\mathcal{R}_{ji}|}$$

where \mathcal{R}_{ji} denotes the set of relations from v_j to v_i . We update an entity representation vector of v_i by

$$\mathbf{h}_i^{(l+1)} = \sigma \left(\beta_{ii}^{(l)} \bar{\mathbf{z}}_i^{(L)} [\mathbf{h}_i^{(l)} \| \bar{\mathbf{z}}_i^{(L)}] + \sum_{v_j \in \mathcal{N}_i} \sum_{r_k \in \mathcal{R}_{ji}} \beta_{ijk}^{(l)} \bar{\mathbf{W}}^{(l)} [\mathbf{h}_j^{(l)} \| \mathbf{z}_k^{(L)}] \right) \quad (4)$$

where $\bar{\mathbf{W}}^{(l)} \in \mathbb{R}^{\hat{d}^l \times (\hat{d}^l + d^l)}$ is a weight matrix, and $\beta_{ii}^{(l)}$ and

$\beta_{ijk}^{(l)}$ are the attention coefficients which are defined by

$$\begin{aligned} \beta_{ii}^{(l)} &= \frac{\exp(\hat{\mathbf{y}}^{(l)} \sigma(\hat{\mathbf{P}}^{(l)} \mathbf{b}_{ii}^{(l)}))}{\exp(\hat{\mathbf{y}}^{(l)} \sigma(\hat{\mathbf{P}}^{(l)} \mathbf{b}_{ii}^{(l)})) + \sum_{v_{j'} \in \mathcal{N}_i} \sum_{r_{k'} \in \mathcal{R}_{j'i}} \exp(\hat{\mathbf{y}}^{(l)} \sigma(\hat{\mathbf{P}}^{(l)} \mathbf{b}_{ij'k'}^{(l)}))}, \\ \beta_{ijk}^{(l)} &= \frac{\exp(\hat{\mathbf{y}}^{(l)} \sigma(\hat{\mathbf{P}}^{(l)} \mathbf{b}_{ijk}^{(l)}))}{\exp(\hat{\mathbf{y}}^{(l)} \sigma(\hat{\mathbf{P}}^{(l)} \mathbf{b}_{ii}^{(l)})) + \sum_{v_{j'} \in \mathcal{N}_i} \sum_{r_{k'} \in \mathcal{R}_{j'i}} \exp(\hat{\mathbf{y}}^{(l)} \sigma(\hat{\mathbf{P}}^{(l)} \mathbf{b}_{ij'k'}^{(l)}))} \end{aligned}$$

where $\mathbf{b}_{ii}^{(l)} = [\mathbf{h}_i^{(l)} \| \mathbf{h}_i^{(l)} \| \bar{\mathbf{z}}_i^{(L)}]$, $\mathbf{b}_{ijk}^{(l)} = [\mathbf{h}_i^{(l)} \| \mathbf{h}_j^{(l)} \| \mathbf{z}_k^{(L)}]$, $\hat{\mathbf{P}}^{(l)} \in \mathbb{R}^{\hat{d}^l \times (2\hat{d}^l + d^l)}$ is a linear transformation matrix, and $\hat{\mathbf{y}}^{(l)} \in \mathbb{R}^{1 \times \hat{d}^l}$ is a row weight vector. We also implement the residual connection and the multi-heads with \hat{K} heads. Our formulation in (4) seamlessly extends GATv2 (Brody et al., 2022) by incorporating the relation representation vectors in every aggregation step. Specifically, when we regard all relation vectors as constant, (4) is equivalent to GATv2. By updating $\mathbf{h}_i^{(l)}$ for $l = 0, \dots, \hat{L}-1$ using (4), we have the final-level entity representation vectors $\mathbf{h}_i^{(\hat{L})}$ ($i = 1, \dots, n$) which are utilized to model relation-entity interactions.

5.3. Modeling Relation-Entity Interactions

Given the representation vectors provided in Section 5.1 and Section 5.2, we compute the final embedding vectors: $\mathbf{z}_k := \mathbf{M}\mathbf{z}_k^{(L)}$ ($k = 1, \dots, m$) for relations and $\mathbf{h}_i := \hat{\mathbf{M}}\mathbf{h}_i^{(\hat{L})}$ ($i = 1, \dots, n$) for entities, where $\mathbf{M} \in \mathbb{R}^{d \times d^l}$ and $\hat{\mathbf{M}} \in \mathbb{R}^{\hat{d} \times \hat{d}^l}$ are trainable projection matrices.

A knowledge graph embedding scoring function, denoted by $f(v_i, r_k, v_j)$, returns a scalar value representing the plausibility of a given triplet (v_i, r_k, v_j) (Schlichtkrull et al., 2018). To model the interactions between relation and entity embeddings, we use a variant of DistMult (Yang et al., 2015). We define our scoring function by

$$f(v_i, r_k, v_j) := \mathbf{h}_i^T \text{diag}(\bar{\mathbf{W}}\mathbf{z}_k)\mathbf{h}_j \quad (5)$$

where $\bar{\mathbf{W}} \in \mathbb{R}^{\hat{d} \times d}$ is a weight matrix that converts the dimension of \mathbf{z}_k from d to \hat{d} and $\text{diag}(\bar{\mathbf{W}}\mathbf{z}_k)$ is the diagonal matrix whose diagonal is defined by $\bar{\mathbf{W}}\mathbf{z}_k$. Let $(v_i, r_k, v_j) \in \mathcal{T}_{\text{tr}}$ be a positive triplet in a training set \mathcal{T}_{tr} described in Section 3. We create negative triplets by corrupting a head or a tail entity of a positive triplet. Let $(\hat{v}_i, r_k, \hat{v}_j) \in \mathcal{T}_{\text{tr}}$ denote the negative triplets. The margin-based ranking loss is defined by

$$\sum_{(v_i, r_k, v_j) \in \mathcal{T}_{\text{tr}}} \sum_{(\hat{v}_i, r_k, \hat{v}_j) \in \mathcal{T}_{\text{tr}}} \max(0, \gamma - f(v_i, r_k, v_j) + f(\hat{v}_i, r_k, \hat{v}_j))$$

where γ is a margin separating the positive and negative triplets. The model parameters are learned by optimizing

the above loss using stochastic gradient descent with a mini-batch based on the Adam optimizer.

5.4. Training Regime

Given $\widetilde{G}_{\text{tr}} = (\mathcal{V}_{\text{tr}}, \mathcal{R}_{\text{tr}}, \mathcal{E}_{\text{tr}})$, we divide \mathcal{E}_{tr} into \mathcal{F}_{tr} and \mathcal{T}_{tr} with a ratio of 3:1. For every epoch, we randomly re-split \mathcal{F}_{tr} and \mathcal{T}_{tr} with the minimal constraint that \mathcal{F}_{tr} includes the minimum spanning tree of $\widetilde{G}_{\text{tr}}$ and \mathcal{F}_{tr} covers all relations in \mathcal{R}_{tr} so that all entity and relation embedding vectors are appropriately learned. At the beginning of each epoch, we initialize all feature vectors using Glorot initialization.

This dynamic split and re-initialization strategy allows INGRAM to robustly learn the model parameters, which makes the model more easily generalizable to an inference graph. In Section 6.4, we empirically observe the importance of dynamic split by the ablation study of INGRAM. Since we randomly re-initialize all feature vectors per epoch during training, INGRAM learns how to compute embedding vectors using random feature vectors, and this is beneficial for computing embeddings with random features at inference time. This observation is consistent with recent studies in (Abboud et al., 2021; Sato et al., 2021) showing that the expressive power of GNNs can be enhanced with randomized initial node features. However, (Abboud et al., 2021; Sato et al., 2021) have analyzed GNNs for standard graphs but not for knowledge graphs. We will further investigate the effects of the combination of dynamic split and random re-initialization strategy from a theoretical point of view.

5.5. Embedding of New Relations and Entities

Given $G_{\text{inf}} = (\mathcal{V}_{\text{inf}}, \mathcal{R}_{\text{inf}}, \mathcal{F}_{\text{inf}})$, we create the relation graph discussed in Section 4 and compute the relation and entity embedding vectors using the learned model parameters of INGRAM. Algorithm 1 shows the overall procedure. Based on the generated embedding vectors of entities and relations on G_{inf} , we can predict missing triplets. For example, to solve $(v_i, r_k, ?)$, we plug each entity $v_j \in \mathcal{V}_{\text{inf}}$ into the given triplet and compute the score using (5) where \overline{W} is already trained during training. The missing entity is predicted to be the one with the highest score.

6. Experimental Results

We compare the performance of INGRAM with other inductive knowledge graph completion methods.

6.1. Datasets and Baseline Methods

Since existing datasets do not contain new relations at $\widetilde{G}_{\text{inf}}$, we create 12 datasets using three benchmarks, NELL-995 (Xiong et al., 2017), Wikidata68K (Gesese et al., 2022), and FB15K237 (Toutanova & Chen, 2015). Let us call these

Algorithm 1 Embeddings via INGRAM at Inference Time

Input: $G_{\text{inf}} = (\mathcal{V}_{\text{inf}}, \mathcal{R}_{\text{inf}}, \mathcal{F}_{\text{inf}})$, the trained model parameters: \mathbf{H} , $\mathbf{W}^{(l)}$, $\mathbf{P}^{(l)}$, $\mathbf{y}^{(l)}$, $c_1^{(l)}, \dots, c_B^{(l)}$ for $l = 0, \dots, L-1$, $\widehat{\mathbf{H}}$, $\widehat{\mathbf{W}}^{(\widehat{l})}$, $\widehat{\mathbf{P}}^{(\widehat{l})}$, $\widehat{\mathbf{y}}^{(\widehat{l})}$, $\widehat{l} = 0, \dots, \widehat{L}-1$, \mathbf{M} , $\widehat{\mathbf{M}}$
Output: \mathbf{z}_i for all $r_i \in \mathcal{R}_{\text{inf}}$ and \mathbf{h}_j for all $v_j \in \mathcal{V}_{\text{inf}}$

- 1: Create the relation graph \mathbf{A} as discussed in Section 4.
- 2: Initialize \mathbf{x}_i for all $r_i \in \mathcal{R}_{\text{inf}}$ and $\widehat{\mathbf{x}}_j$ for all $v_j \in \mathcal{V}_{\text{inf}}$ using Glorot initialization.
- 3: Set $\mathbf{z}_i^{(0)} \leftarrow \mathbf{Hx}_i$ and $\mathbf{h}_j^{(0)} \leftarrow \widehat{\mathbf{H}}\widehat{\mathbf{x}}_j$.
- 4: **for** $l = 0, \dots, L-1$ **do**
- 5: **for** $r_i \in \mathcal{R}_{\text{inf}}$ **do**
- 6: Compute $\mathbf{z}_i^{(l+1)}$ according to (1) using $\mathbf{W}^{(l)}$, $\mathbf{P}^{(l)}$, $\mathbf{y}^{(l)}$, and $c_1^{(l)}, \dots, c_B^{(l)}$.
- 7: **end for**
- 8: **end for**
- 9: **for** $l = 0, \dots, \widehat{L}-1$ **do**
- 10: **for** $v_j \in \mathcal{V}_{\text{inf}}$ **do**
- 11: Compute $\mathbf{h}_j^{(l+1)}$ according to (4) using $\widehat{\mathbf{W}}^{(l)}$, $\widehat{\mathbf{P}}^{(l)}$, $\widehat{\mathbf{y}}^{(l)}$, and $\mathbf{z}_i^{(L)}$ for $r_i \in \mathcal{R}_{\text{inf}}$.
- 12: **end for**
- 13: **end for**
- 14: $\mathbf{z}_i \leftarrow \mathbf{Mz}_i^{(L)}$ for $r_i \in \mathcal{R}_{\text{inf}}$ and $\mathbf{h}_j \leftarrow \widehat{\mathbf{M}}\mathbf{h}_j^{(\widehat{L})}$ for $v_j \in \mathcal{V}_{\text{inf}}$.

benchmarks NL, WK, and FB, respectively. For each benchmark, we create four datasets by varying the percentage of triplets with new relations: 100%, 75%, 50% and 25%. For example, in NL-75, approximately 75% of triplets have new relations, and 25% of triplets have known relations, i.e., semi-inductive inference for relations. On the other hand, in NL-100, all triplets have new relations, i.e., inductive inference for relations. In all 12 datasets, all entities in $\widetilde{G}_{\text{inf}}$ are new entities, as also assumed in (Teru et al., 2020). Details about these datasets are described in Appendix A.

We compare the performance of INGRAM with 14 different methods: GraIL (Teru et al., 2020), CoMPILE (Mai et al., 2021), SNRI (Xu et al., 2022), INDIGO (Liu et al., 2021), RMPI (Geng et al., 2023), CompGCN (Vashishth et al., 2020), NodePiece (Galkin et al., 2022), NeuralLP (Yang et al., 2017), DRUM (Sadeghian et al., 2019), BLP (Daza et al., 2021), QBLP (Ali et al., 2021), NBFNet (Zhu et al., 2021), RED-GNN (Zhang & Yao, 2022), and RAILD (Gesese et al., 2022).

Since the original implementations of GraIL, CoMPILE, SNRI, INDIGO, and RMPI were based on subgraph sampling, we extended them to consider all entities in \mathcal{V}_{inf} to evaluate the performance more accurately. Due to the scalability issues of GraIL, CoMPILE, SNRI, INDIGO, and RMPI, they only run on NL datasets. BLP, QBLP and RAILD require BERT-based pre-trained vectors which are produced based on the names and textual descriptions of entities or relations. We provide BLP, QBLP and RAILD with the pre-trained vectors using available information. Since

Table 1: Inductive link prediction performance on 12 different datasets, where all entities are new, whereas the last digits of each dataset (100, 75, 50, and 25) indicate the ratio of new relations. The best results are boldfaced and the second-best results are underlined. Our model, INGRAM, significantly outperforms the baseline methods in most cases.

| | NL-100 | | | | NL-75 | | | | NL-50 | | | | NL-25 | | | |
|-----------|---------------|--------------|--------------|--------------|--------------|--------------|--------------|--------------|---------------|--------------|--------------|--------------|--------------|--------------|--------------|--------------|
| | MR | MRR | Hit@10 | Hit@1 | MR | MRR | Hit@10 | Hit@1 | MR | MRR | Hit@10 | Hit@1 | MR | MRR | Hit@10 | Hit@1 |
| Grail | 928.4 | 0.135 | 0.173 | 0.114 | 526.0 | 0.096 | 0.205 | 0.036 | 837.6 | 0.162 | 0.288 | 0.104 | 692.9 | 0.216 | 0.366 | 0.160 |
| CoMPILE | 743.1 | 0.123 | 0.209 | 0.071 | 519.6 | 0.178 | <u>0.361</u> | 0.093 | 466.6 | 0.194 | 0.330 | 0.125 | 438.9 | 0.189 | 0.324 | 0.115 |
| SNRI | 809.8 | 0.042 | 0.064 | 0.029 | 418.7 | 0.088 | 0.177 | 0.040 | 584.6 | 0.130 | 0.187 | 0.095 | 417.7 | 0.190 | 0.270 | 0.140 |
| INDIGO | 621.1 | 0.160 | 0.247 | 0.109 | 587.4 | 0.121 | 0.156 | 0.098 | 864.9 | 0.167 | 0.217 | 0.134 | 812.4 | 0.166 | 0.206 | 0.134 |
| RMPI | <u>143.9</u> | <u>0.220</u> | 0.376 | <u>0.136</u> | 244.5 | 0.138 | 0.275 | 0.061 | 479.1 | 0.185 | 0.307 | 0.109 | 385.7 | 0.213 | 0.329 | 0.130 |
| CompGCN | 877.9 | 0.008 | 0.014 | 0.001 | 750.5 | 0.014 | 0.025 | 0.003 | 1183.6 | 0.003 | 0.005 | 0.000 | 1052.5 | 0.006 | 0.010 | 0.000 |
| NodePiece | 755.1 | 0.012 | 0.018 | 0.004 | 565.8 | 0.042 | 0.081 | 0.020 | 832.2 | 0.037 | 0.079 | 0.013 | 620.9 | 0.098 | 0.166 | 0.057 |
| NeuralLP | 530.3 | 0.084 | 0.181 | 0.035 | 447.3 | 0.117 | 0.273 | 0.048 | 802.4 | 0.101 | 0.190 | 0.064 | 631.8 | 0.148 | 0.271 | 0.101 |
| DRUM | 532.6 | 0.076 | 0.138 | 0.044 | 445.4 | 0.152 | 0.313 | 0.072 | 803.8 | 0.107 | 0.193 | 0.070 | 637.1 | 0.161 | 0.264 | 0.119 |
| BLP | 564.8 | 0.019 | 0.037 | 0.006 | <u>242.5</u> | 0.051 | 0.120 | 0.012 | 426.5 | 0.041 | 0.093 | 0.011 | 332.9 | 0.049 | 0.095 | 0.024 |
| QBLP | 754.6 | 0.004 | 0.003 | 0.000 | 258.8 | 0.040 | 0.095 | 0.007 | 383.6 | 0.048 | 0.097 | 0.020 | <u>287.2</u> | 0.073 | 0.151 | 0.027 |
| NBFNet | 208.2 | 0.096 | 0.199 | 0.032 | 256.2 | 0.137 | 0.255 | 0.077 | <u>332.0</u> | <u>0.225</u> | <u>0.346</u> | <u>0.161</u> | 421.8 | <u>0.283</u> | <u>0.417</u> | <u>0.224</u> |
| RED-GNN | 201.7 | 0.212 | <u>0.385</u> | 0.114 | 470.1 | <u>0.203</u> | 0.353 | <u>0.129</u> | 622.5 | 0.179 | 0.280 | 0.115 | 403.0 | 0.214 | 0.266 | 0.166 |
| RAILD | 598.1 | 0.018 | 0.037 | 0.005 | N/A | N/A | N/A | N/A | N/A | N/A | N/A | N/A | N/A | N/A | N/A | N/A |
| INGRAM | 92.6 | 0.309 | 0.506 | 0.212 | 59.1 | 0.261 | 0.464 | 0.167 | 105.1 | 0.281 | 0.453 | 0.193 | 90.1 | 0.334 | 0.501 | 0.241 |
| | WK-100 | | | | WK-75 | | | | WK-50 | | | | WK-25 | | | |
| | MR | MRR | Hit@10 | Hit@1 | MR | MRR | Hit@10 | Hit@1 | MR | MRR | Hit@10 | Hit@1 | MR | MRR | Hit@10 | Hit@1 |
| CompGCN | 5861.5 | 0.003 | 0.009 | 0.000 | 1265.1 | 0.015 | 0.028 | 0.003 | 3297.4 | 0.003 | 0.002 | 0.001 | 1591.7 | 0.009 | 0.020 | 0.000 |
| NodePiece | 5334.1 | 0.007 | 0.018 | 0.002 | 800.3 | 0.021 | 0.052 | 0.003 | 3256.4 | 0.008 | 0.013 | 0.002 | 814.5 | 0.053 | 0.122 | 0.019 |
| NeuralLP | 5665.5 | 0.009 | 0.016 | 0.005 | 1191.5 | 0.020 | 0.054 | 0.004 | 4160.8 | 0.025 | 0.054 | 0.007 | 1384.1 | 0.068 | 0.104 | 0.046 |
| DRUM | 5668.0 | 0.010 | 0.019 | 0.004 | 1192.1 | 0.020 | 0.043 | 0.007 | 4163.0 | 0.017 | 0.046 | 0.002 | 1383.2 | 0.064 | 0.116 | 0.035 |
| BLP | 3888.1 | 0.012 | 0.025 | 0.003 | <u>523.9</u> | 0.043 | 0.089 | 0.016 | 1625.7 | 0.041 | 0.092 | 0.013 | 175.4 | 0.125 | 0.283 | 0.055 |
| QBLP | 2863.1 | 0.012 | 0.025 | 0.003 | 555.0 | 0.044 | 0.091 | 0.016 | 1371.4 | 0.035 | 0.080 | 0.011 | 342.0 | 0.116 | 0.294 | 0.042 |
| NBFNet | 4030.3 | 0.014 | 0.026 | 0.005 | 548.1 | 0.072 | 0.172 | 0.028 | 2874.0 | <u>0.062</u> | <u>0.105</u> | 0.036 | 790.5 | 0.154 | <u>0.301</u> | 0.092 |
| RED-GNN | 5382.4 | <u>0.096</u> | <u>0.136</u> | <u>0.070</u> | 906.2 | <u>0.172</u> | <u>0.290</u> | <u>0.110</u> | 3198.3 | 0.058 | 0.093 | 0.033 | 769.2 | <u>0.170</u> | 0.263 | <u>0.111</u> |
| RAILD | 2005.6 | 0.026 | 0.052 | 0.010 | N/A | N/A | N/A | N/A | N/A | N/A | N/A | N/A | N/A | N/A | N/A | N/A |
| INGRAM | 1515.7 | 0.107 | 0.169 | 0.072 | 315.5 | 0.247 | 0.362 | 0.179 | <u>1374.1</u> | 0.068 | 0.135 | <u>0.034</u> | <u>263.8</u> | 0.186 | 0.309 | 0.124 |
| | FB-100 | | | | FB-75 | | | | FB-50 | | | | FB-25 | | | |
| | MR | MRR | Hit@10 | Hit@1 | MR | MRR | Hit@10 | Hit@1 | MR | MRR | Hit@10 | Hit@1 | MR | MRR | Hit@10 | Hit@1 |
| CompGCN | 1201.2 | 0.015 | 0.025 | 0.008 | 1211.6 | 0.013 | 0.026 | 0.000 | 2193.1 | 0.004 | 0.006 | 0.002 | 1957.4 | 0.003 | 0.004 | 0.000 |
| NodePiece | 1131.3 | 0.006 | 0.009 | 0.001 | 1162.7 | 0.016 | 0.029 | 0.007 | 1314.3 | 0.021 | 0.048 | 0.006 | 916.3 | 0.044 | 0.114 | 0.011 |
| NeuralLP | 988.2 | 0.026 | 0.057 | 0.007 | 855.0 | 0.056 | 0.099 | 0.030 | 1501.9 | 0.088 | 0.184 | 0.043 | 997.8 | 0.164 | 0.309 | 0.098 |
| DRUM | 984.0 | 0.034 | 0.077 | 0.011 | 853.8 | 0.065 | 0.121 | 0.034 | 1490.2 | 0.101 | 0.191 | 0.061 | 992.5 | 0.175 | 0.320 | 0.109 |
| BLP | 913.1 | 0.017 | 0.035 | 0.004 | <u>705.1</u> | 0.047 | 0.085 | 0.024 | 588.5 | 0.078 | 0.156 | 0.037 | 384.5 | 0.107 | 0.212 | 0.053 |
| QBLP | 842.8 | 0.013 | 0.026 | 0.003 | 798.3 | 0.041 | 0.084 | 0.017 | 564.9 | 0.071 | 0.147 | 0.030 | <u>352.6</u> | 0.104 | 0.226 | 0.043 |
| NBFNet | 451.5 | 0.072 | 0.154 | 0.026 | 550.8 | 0.089 | 0.166 | 0.048 | 758.5 | <u>0.130</u> | <u>0.259</u> | <u>0.071</u> | 571.4 | 0.224 | 0.410 | <u>0.137</u> |
| RED-GNN | <u>375.6</u> | <u>0.121</u> | <u>0.263</u> | <u>0.053</u> | 890.0 | <u>0.107</u> | <u>0.201</u> | <u>0.057</u> | 1169.3 | <u>0.129</u> | <u>0.251</u> | 0.072 | 1234.1 | 0.145 | 0.284 | 0.077 |
| RAILD | 686.0 | 0.031 | 0.048 | 0.016 | N/A | N/A | N/A | N/A | N/A | N/A | N/A | N/A | N/A | N/A | N/A | N/A |
| INGRAM | 171.5 | 0.223 | 0.371 | 0.146 | 217.4 | 0.189 | 0.325 | 0.119 | <u>580.2</u> | 0.117 | 0.218 | 0.067 | 330.3 | 0.133 | 0.271 | 0.067 |

RAILD is not implemented for the case where both known and new relations are present at inference time, we could not report the results of RAILD for the 75%, 50% and 25% settings. We provide the same training graph for all methods. Given \mathcal{E}_{tr} , how to use \mathcal{E}_{tr} depends on each method. For example, Grail uses the entire \mathcal{E}_{tr} for training without any split. In INGRAM, we use the dynamic split scheme as described in Section 5.4. For a fair comparison, we feed \mathcal{F}_{inf} , \mathcal{T}_{val} and \mathcal{T}_{test} to all baselines exactly in the same way INGRAM uses. More details about how we run the baseline methods are described in Appendix B.

We set $d = 32$ and $\hat{d} = 32$ for INGRAM and all the baseline methods. Note that we initialize the initial features of relations and entities (\mathbf{x}_i in Section 5.1 and $\hat{\mathbf{x}}_i$ in Section 5.2) using Glorot initialization in INGRAM. Details about how we tune the hyperparameters of INGRAM are described in Appendix C.

6.2. Inductive Link Prediction

We measure the inductive link prediction performance of the methods using standard metrics (Wang et al., 2017): MR (↓), MRR (↑), Hit@10 (↑), and Hit@1 (↑). Table 1 shows the results on 12 different datasets, where all entities are new, and each dataset has a different ratio of new relations. Among the 12 datasets, NL-100, WK-100, and FB-100 have entirely new relations (i.e., inductive inference for relations), whereas the other 9 datasets contain a mixture of new and known relations (i.e., semi-inductive inference for relations). In Table 1, we first note that INGRAM significantly outperforms all the baseline methods in NL-100, WK-100, and FB-100, which are the most challenging datasets since relations and entities are all new. In these datasets, the performance gap between INGRAM and the best baseline method is considerable in terms of all metrics. This shows that INGRAM is the most effective method for inductive inference for relations.

Table 2: Inductive link prediction performance of known relations and new relations on NL-50.

| | Known Relations | | | New Relations | | |
|-----------|-----------------|--------------|--------------|---------------|--------------|--------------|
| | MR | MRR | Hit@10 | MR | MRR | Hit@10 |
| GraIL | 711.8 | 0.264 | 0.389 | 936.0 | 0.082 | 0.209 |
| CoMPILE | 418.0 | 0.250 | 0.383 | 504.6 | 0.150 | 0.288 |
| SNRI | 515.8 | 0.206 | 0.240 | 638.4 | 0.071 | 0.146 |
| INDIGO | 943.6 | 0.185 | 0.264 | 803.4 | 0.152 | 0.180 |
| RMPI | 492.8 | 0.192 | 0.312 | 468.4 | 0.180 | 0.304 |
| CompGCN | 1195.6 | 0.004 | 0.005 | 1174.2 | 0.003 | 0.004 |
| NodePiece | 575.6 | 0.067 | 0.151 | 1033.5 | 0.016 | 0.039 |
| NeuralLP | 784.5 | 0.147 | 0.204 | 816.3 | 0.065 | 0.180 |
| DRUM | 787.8 | 0.146 | 0.196 | 816.4 | 0.076 | 0.191 |
| BLP | 357.1 | 0.056 | 0.131 | 480.8 | 0.030 | 0.062 |
| QBLP | 271.2 | 0.073 | 0.142 | 471.4 | 0.029 | 0.061 |
| NBFNet | 317.4 | 0.231 | 0.353 | 350.7 | 0.217 | 0.338 |
| RED-GNN | 565.3 | 0.210 | 0.300 | 667.2 | 0.154 | 0.265 |
| INGRAM | 100.7 | 0.330 | 0.481 | 108.5 | 0.244 | 0.430 |

Let us now consider the semi-inductive inference settings. In all NL and WK datasets as well as FB-75 datasets, INGRAM significantly outperforms the baseline methods. We also note that the performance gap between INGRAM and the baseline methods becomes more prominent when the ratio of new relations increases.

While INGRAM shows clearly better performance than the baseline methods on 10 out of 12 datasets, some baseline methods such as NBFNet and RED-GNN show better performance than INGRAM on FB-25 and FB-50. Indeed, we notice that there exist simple rules between known relations in these datasets, and thus, even a simple rule-based prediction works well on these datasets. This partly explains the performance of NeuralLP, DRUM, RED-GNN, and NBFNet, which are designed to capture rules or patterns between known relations and directly apply them at inference time. Different from these methods, INGRAM does not memorize particular patterns between known relations; instead, INGRAM focuses more on generalizability which is more beneficial for generating embeddings of new relations.

In Table 2, we analyze the model performances on triplets with known relations and new relations on NL-50. All methods perform better on known relations than new relations. Also, for the baseline methods, the performance gaps between known and new relations are substantial. We see that the performance of INGRAM is much better than the best baseline methods in all metrics for both known and new relations.

6.3. Inductive Link Prediction with Known Relations

Even though INGRAM is designed to consider the case where new relations appear at inference time, we also conduct experiments on the conventional inductive link prediction scenario where all relations are known and all entities are new (Teru et al., 2020). We create a dataset NL-0 that satisfies this constraint, where $|\mathcal{V}_{\text{tr}}| = 1,814$, $|\mathcal{R}_{\text{tr}}| = 134$,

Table 3: Inductive link prediction on NL-0 and NELL-995-v1, where all relations are known and all entities are new.

| | MR | MRR | Hit@10 | Hit@1 |
|-------------|-----------|--------------|--------------|--------------|
| NL-0 | GraIL | 508.2 | 0.192 | 0.332 |
| | CoMPILE | 561.4 | 0.229 | 0.381 |
| | SNRI | 561.3 | 0.117 | 0.176 |
| | INDIGO | 705.6 | 0.201 | 0.263 |
| | RMPI | 396.1 | 0.225 | 0.339 |
| | CompGCN | 954.3 | 0.005 | 0.009 |
| | NodePiece | 345.2 | 0.094 | 0.210 |
| | NeuralLP | 566.3 | 0.175 | 0.326 |
| | DRUM | 565.9 | 0.200 | 0.343 |
| | BLP | 467.2 | 0.044 | 0.100 |
| | QBLP | 346.2 | 0.060 | 0.144 |
| | NBFNet | 160.2 | 0.263 | 0.430 |
| NELL-995-v1 | RED-GNN | 330.9 | 0.222 | 0.368 |
| | RAILD | 468.4 | 0.050 | 0.109 |
| | INGRAM | 152.4 | 0.269 | 0.431 |
| | GraIL | 18.7 | 0.499 | 0.595 |
| | CoMPILE | 20.1 | 0.474 | 0.575 |
| | SNRI | 21.2 | 0.419 | 0.520 |
| | INDIGO | 20.4 | 0.521 | 0.595 |
| | RMPI | 50.3 | 0.484 | 0.545 |
| | CompGCN | 11.8 | 0.282 | 0.750 |
| | NodePiece | 9.8 | 0.677 | 0.885 |
| | NeuralLP | 33.0 | 0.547 | 0.785 |
| | DRUM | 33.4 | 0.536 | 0.760 |

$|\mathcal{E}_{\text{tr}}| = 7,796$ and $|\mathcal{V}_{\text{inf}}| = 2,026$, $|\mathcal{R}_{\text{inf}}| = 112$, $|\mathcal{E}_{\text{inf}}| = 3,813$. We call this dataset NL-0 since it includes 0% new relations.

Also, we take an existing benchmark dataset, NELL-995-v1, from (Teru et al., 2020). We note that different papers did experiments under different settings, even though they used the same benchmark dataset. We conduct our experiments in a setting consistent with our other experiments. For the results on NELL-995-v1, our reproduced results can differ from those reported in the previous literature for the following reasons: (i) we use the validation set inside the “ind-test” set provided in NELL-995-v1, (ii) when measuring the link prediction performance, we use the test set of “ind-test”, (iii) for a fair comparison, we set the embedding dimension to 32 for all methods, and (iv) when conducting link prediction, we set the candidate set to be the entire entity set of the inference graph.

Table 3 shows the inductive link prediction results on NL-0 and NELL-995-v1, where all entities are new and all relations are known. We see that INGRAM outperforms all baselines in all metrics. Even though INGRAM does not learn relation-specific patterns as other baselines do, INGRAM shows reasonable performance on transductive inference for relations while having extra generalization capability to semi-inductive and inductive inferences for relations.

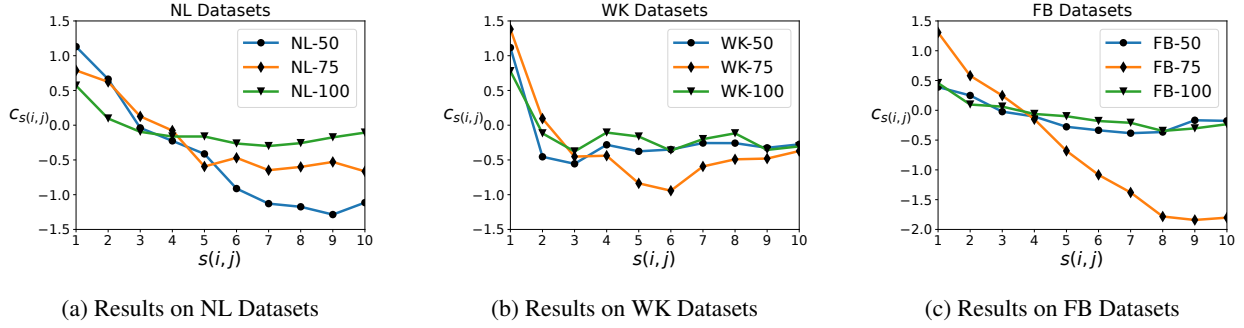


Figure 4: Visualization of the $c_{s(i,j)}$ values learned by INGRAM with $B = 10$. The $c_{s(i,j)}$ value is expected to be large for a small $s(i,j)$, and small for a large $s(i,j)$. See Section 5.1 for more details.

Table 4: Ablation Studies of INGRAM.

| | NL-100 | | WK-100 | | FB-100 | |
|---------------------|--------|--------|--------|--------|--------|--------|
| | MRR | Hit@10 | MRR | Hit@10 | MRR | Hit@10 |
| w/ mean aggregator | 0.259 | 0.421 | 0.047 | 0.106 | 0.110 | 0.184 |
| w/ sum aggregator | 0.049 | 0.082 | 0.000 | 0.000 | 0.001 | 0.000 |
| w/ self-loop vector | 0.133 | 0.292 | 0.007 | 0.015 | 0.014 | 0.027 |
| w/o dynamic split | 0.234 | 0.418 | 0.036 | 0.100 | 0.134 | 0.271 |
| w/o relation update | 0.235 | 0.415 | 0.057 | 0.138 | 0.183 | 0.310 |
| w/o binning | 0.209 | 0.443 | 0.070 | 0.138 | 0.142 | 0.292 |
| INGRAM | 0.309 | 0.506 | 0.107 | 0.169 | 0.223 | 0.371 |

6.4. Ablation Studies of INGRAM

We conduct ablation studies for INGRAM to validate the importance of each module of INGRAM. Specifically, we compare the performance of INGRAM under the following settings: (i) we replace the attention-based aggregation in (1) and (4) with the mean aggregator or (ii) the sum aggregator; (iii) when we update an entity representation in (4), we replace $\bar{z}_i^{(L)}$ with a separate learnable self-loop vector as in (Vashisht et al., 2020); (iv) we do not dynamically re-split \mathcal{F}_{tr} and \mathcal{T}_{tr} as described in Section 5.4, i.e., we fix the split during training; (v) we do not update a relation representation vector; (vi) we set $B = 1$ in (3), i.e., we do not utilize the affinity weights in updating relation representations. The results of these settings are shown in Table 4 in order. Removing each module leads to a noticeable degradation in the performance of INGRAM. While some are more critical and others are less, INGRAM achieves the best performance when all modules come together.

6.5. Qualitative Analysis of INGRAM

In Section 5.1, when updating the relation vectors using (2), we introduce the learnable parameters $c_{s(i,j)}$ for computing the attention coefficient between r_i and r_j . By definition of $s(i,j)$ in (3), the value of $s(i,j)$ is small if r_i and r_j are similar. Since we expect that two similar relations have a high attention value, we expect that $c_{s(i,j)}$ is large for a small $s(i,j)$, and $c_{s(i,j)}$ is small for a large $s(i,j)$. Figure 4 shows

the learned $c_{s(i,j)}$ values according to $s(i,j)$. Even though some exceptions exist, overall, the plots are going down from left to right; the $c_{s(i,j)}$ values are learned as expected. Indeed, when we tune the number of bins $B \in \{1, 5, 10\}$, INGRAM achieves the best performance when $B = 10$, showing the advantage of differentiating bins.

7. Conclusion and Future Work

We consider challenging and realistic inductive learning scenarios where new entities accompany new relations. Our method, INGRAM, can generate embeddings of new relations and entities only appearing at inference time. INGRAM conducts inferences based only on the structure of a given knowledge graph without any extra information about the entities and relations or the aid of rich language models.

While existing methods are biased toward learning the patterns of known relations, INGRAM focuses more on the generalization capability useful for modeling new relations. We will investigate the ways in which INGRAM can incorporate known-relation-specific patterns into inferences when known relations are dominant. We also plan to do the theoretical analysis of INGRAM as done in (Xu et al., 2019), (Barcelo et al., 2022) and (Hamilton et al., 2017), as well as consider some extensions to hyper-relational facts (Chung et al., 2023) and bi-level or hierarchical structures (Chung & Whang, 2023; Kwak et al., 2022). Finally, we will look into how we can make the predictions of INGRAM robust and reliable to possibly noisy information (Hong et al., 2023) in a given knowledge graph.

Acknowledgements

This research was supported by an NRF grant funded by MSIT 2022R1A2C4001594 (Extendable Graph Representation Learning) and an IITP grant funded by MSIT 2022-0-00369 (Development of AI Technology to support Expert Decision-making that can Explain the Reasons/Grounds for Judgment Results based on Expert Knowledge).

References

Abboud, R., Ceylan, İ. İ., Grohe, M., and Lukasiewicz, T. The surprising power of graph neural networks with random node initialization. In *Proceedings of the 30th International Joint Conference on Artificial Intelligence*, pp. 2112–2118, 2021.

Ali, M., Berrendorf, M., Galkin, M., Thost, V., Ma, T., Tresp, V., and Lehmann, J. Improving inductive link prediction using hyper-relational facts. In *Proceedings of the 20th International Semantic Web Conference*, pp. 74–92, 2021.

Barcelo, P., Galkin, M., Morris, C., and Orth, M. R. Weisfeiler and Leman go relational. In *Proceedings of the 1st Learning on Graphs Conference*, 2022.

Brody, S., Alon, U., and Yahav, E. How attentive are graph attention networks? In *Proceedings of the 10th International Conference on Learning Representations*, 2022.

Chen, J., He, H., Wu, F., and Wang, J. Topology-aware correlations between relations for inductive link prediction in knowledge graphs. In *Proceedings of the 35th AAAI Conference on Artificial Intelligence*, pp. 6271–6278, 2021.

Chung, C. and Whang, J. J. Learning representations of bi-level knowledge graphs for reasoning beyond link prediction. In *arXiv preprint*, 2023. doi: 10.48550/arXiv.2302.02601.

Chung, C., Lee, J., and Whang, J. J. Representation learning on hyper-relational and numeric knowledge graphs with transformers. In *arXiv preprint*, 2023. doi: 10.48550/arXiv.2305.18256.

Cui, Y., Wang, Y., Sun, Z., Liu, W., Jiang, Y., Han, K., and Hu, W. Inductive knowledge graph reasoning for multi-batch emerging entities. In *Proceedings of the 31st ACM International Conference on Information and Knowledge Management*, pp. 335–344, 2022.

Dai, D., Zheng, H., Luo, F., Yang, P., Liu, T., Sui, Z., and Chang, B. Inductively representing out-of-knowledge-graph entities by optimal estimation under translational assumptions. In *Proceedings of the 6th Workshop on Representation Learning for NLP*, pp. 83–89, 2021.

Daza, D., Cochez, M., and Groth, P. Inductive entity representations from text via link prediction. In *Proceedings of the Web Conference 2021*, pp. 798–808, 2021.

Devlin, J., Chang, M.-W., Lee, K., and Toutanova, K. BERT: Pre-training of deep bidirectional transformers for language understanding. In *Proceedings of the 2019 Conference of the North American Chapter of the Association for Computational Linguistics: Human Language Technologies*, pp. 4171–4186, 2019.

Galkin, M., Denis, E., Wu, J., and Hamilton, W. L. Node-Piece: Compositional and parameter-efficient representations of large knowledge graphs. In *Proceedings of the 10th International Conference on Learning Representations*, 2022.

Geng, Y., Chen, J., Pan, J. Z., Chen, M., Jiang, S., Zhang, W., and Chen, H. Relational message passing for fully inductive knowledge graph completion. In *Proceedings of the 39th IEEE International Conference on Data Engineering*, 2023.

Gesese, G. A., Sack, H., and Alam, M. RAILD: Towards leveraging relation features for inductive link prediction in knowledge graphs. In *Proceedings of the 11th International Joint Conference on Knowledge Graphs*, 2022.

Glorot, X. and Bengio, Y. Understanding the difficulty of training deep feedforward neural networks. In *Proceedings of the 13th International Conference on Artificial Intelligence and Statistics*, pp. 249–256, 2010.

Hamaguchi, T., Oiwa, H., Shimbo, M., and Matsumoto, Y. Knowledge transfer for out-of-knowledge-base entities: A graph neural network approach. In *Proceedings of the 26th International Joint Conference on Artificial Intelligence*, pp. 1802–1808, 2017.

Hamilton, W. L., Ying, R., and Leskovec, J. Inductive representation learning on large graphs. In *Proceedings of the 31st Conference on Neural Information Processing System*, pp. 1025–1035, 2017.

He, K., Zhang, X., Ren, S., and Sun, J. Deep residual learning for image recognition. In *2016 IEEE Conference on Computer Vision and Pattern Recognition*, pp. 770–778, 2016.

Hong, G., Kim, J., Kang, J., Myaeng, S.-H., and Whang, J. J. Discern and answer: Mitigating the impact of misinformation in retrieval-augmented models with discriminators. In *arXiv preprint*, 2023. doi: 10.48550/arXiv.2305.01579.

Ji, S., Pan, S., Cambria, E., Marttinen, P., and Yu, P. S. A survey on knowledge graphs: Representation, acquisition, and applications. *IEEE Transactions on Neural Networks and Learning Systems*, 33(2):494–514, 2022.

Jin, J., Wang, Y., Du, K., Zhang, W., Zhang, Z., Wipf, D., Yu, Y., and Gan, Q. Inductive relation prediction using analogy subgraph embeddings. In *Proceedings of the 10th International Conference on Learning Representations*, 2022.

Kipf, T. N. and Welling, M. Semi-supervised classification with graph convolutional networks. In *Proceedings of the 5th International Conference on Learning Representations*, 2017.

Kwak, J. H., Lee, J., Whang, J. J., and Jo, S. Semantic grasping via a knowledge graph of robotic manipulation: A graph representation learning approach. *IEEE Robotics and Automation Letters*, 7(4):9397–9404, 2022.

Lin, Q., Liu, J., Xu, F., Pan, Y., Zhu, Y., Zhang, L., and Zhao, T. Incorporating context graph with logical reasoning for inductive relation prediction. In *Proceedings of the 45th International ACM SIGIR Conference on Research and Development in Information Retrieval*, pp. 893–903, 2022.

Liu, H., Wu, Y., and Yang, Y. Analogical inference for multi-relational embeddings. In *Proceedings of the 37th International Conference on Machine Learning*, pp. 2168–2178, 2017.

Liu, S., Grau, B., Horrocks, I., and Kostylev, E. INDIGO: GNN-based inductive knowledge graph completion using pair-wise encoding. In *Proceedings of the 35th Conference on Neural Information Processing Systems*, pp. 2034–2045, 2021.

Maas, A. L., Hannun, A. Y., and Ng, A. Y. Rectifier nonlinearities improve neural network acoustic models. In *ICML 2013 Workshop on Deep Learning for Audio, Speech and Language Processing*, 2013.

Mai, S., Zheng, S., Yang, Y., and Hu, H. Communicative message passing for inductive relation reasoning. In *Proceedings of the 35th AAAI Conference on Artificial Intelligence*, pp. 4294–4302, 2021.

Markowitz, E., Balasubramanian, K., Mirtaheri, M., Annaram, M., Galstyan, A., and Steeg, G. V. StATIK: Structure and text for inductive knowledge graph completion. In *Findings of the Association for Computational Linguistics: NAACL 2022*, pp. 604–615, 2022.

Nathani, D., Chauhan, J., Sharma, C., and Kaul, M. Learning attention-based embeddings for relation prediction in knowledge graphs. In *Proceedings of the 57th Annual Meeting of the Association for Computational Linguistics*, pp. 4710–4723, 2019.

Sadeghian, A., Armandpour, M., patrick Ding, and Wang, D. Z. DRUM: End-to-end differentiable rule mining on knowledge graphs. In *Proceedings of the 33rd Conference on Neural Information Processing Systems*, pp. 15347–15357, 2019.

Sato, R., Yamada, M., and Kashima, H. Random features strengthen graph neural networks. In *Proceedings of the 2021 SIAM International Conference on Data Mining*, pp. 333–341, 2021.

Schlichtkrull, M., Kipf, T. N., Bloem, P., van den Berg, R., Titov, I., and Welling, M. Modeling relational data with graph convolutional networks. In *Proceedings of the 15th International Semantic Web Conference*, pp. 593–607, 2018.

Sun, Z., Deng, Z.-H., Nie, J.-Y., and Tang, J. RotatE: Knowledge graph embedding by relational rotation in complex space. In *Proceedings of the 7th International Conference on Learning Representations*, 2019.

Teru, K., Denis, E., and Hamilton, W. Inductive relation prediction by subgraph reasoning. In *Proceedings of the 37th International Conference on Machine Learning*, pp. 9448–9457, 2020.

Toutanova, K. and Chen, D. Observed versus latent features for knowledge base and text inference. In *Proceedings of the 3rd Workshop on Continuous Vector Space Models and their Compositionality*, pp. 57–66, 2015.

Vashishth, S., Sanyal, S., Nitin, V., and Talukdar, P. Composition-based multi-relational graph convolutional networks. In *Proceedings of the 8th International Conference on Learning Representations*, 2020.

Vaswani, A., Shazeer, N., Parmar, N., Uszkoreit, J., Jones, L., Gomez, A. N., Łukasz Kaiser, and Polosukhin, I. Attention is all you need. In *Proceedings of the 31st Conference on Neural Information Processing Systems*, pp. 5998–6008, 2017.

Veličković, P., Cucurull, G., Casanova, A., Romero, A., Liò, P., and Bengio, Y. Graph attention networks. In *Proceedings of the 6th International Conference on Learning Representations*, 2018.

Wang, C., Zhou, X., Pan, S., Dong, L., Song, Z., and Sha, Y. Exploring relational semantics for inductive knowledge graph completion. In *Proceedings of the 36th AAAI Conference on Artificial Intelligence*, pp. 4184–4192, 2022.

Wang, H., Ren, H., and Leskovec, J. Relational message passing for knowledge graph completion. In *Proceedings of the 27th ACM SIGKDD Conference on Knowledge Discovery and Data Mining*, pp. 1697–1707, 2021.

Wang, P., Han, J., Li, C., and Pan, R. Logic attention based neighborhood aggregation for inductive knowledge graph embedding. In *Proceedings of the 33rd AAAI Conference on Artificial Intelligence*, pp. 7152–7159, 2019.

Wang, Q., Mao, Z., Wang, B., and Guo, L. Knowledge graph embedding: A survey of approaches and applications. *IEEE Transactions on Knowledge and Data Engineering*, 29(12):2724–2743, 2017.

Xiong, W., Hoang, T., and Wang, W. Y. DeepPath: A reinforcement learning method for knowledge graph reasoning. In *Proceedings of the 2017 Conference on Empirical Methods in Natural Language Processing*, pp. 564–573, 2017.

Xu, K., Hu, W., Leskovec, J., and Jegelka, S. How powerful are graph neural networks? In *Proceedings of the 7th International Conference on Learning Representations*, 2019.

Xu, X., Zhang, P., He, Y., Chao, C., and Yan, C. Subgraph neighboring relations infomax for inductive link prediction on knowledge graphs. In *Proceedings of the 31st International Joint Conference on Artificial Intelligence*, pp. 2341–2347, 2022.

Yan, Z., Ma, T., Gao, L., Tang, Z., and Chen, C. Cycle representation learning for inductive relation prediction. In *Proceedings of the 39th International Conference on Machine Learning*, pp. 24895–24910, 2022.

Yang, B., tau Yih, W., He, X., Gao, J., and Deng, L. Embedding entities and relations for learning and inference in knowledge bases. In *Proceedings of the 3rd International Conference on Learning Representations*, 2015.

Yang, F., Yang, Z., and Cohen, W. W. Differentiable learning of logical rules for knowledge base reasoning. In *Proceedings of the 31st Conference on Neural Information Processing Systems*, pp. 2319–2328, 2017.

Ying, C., Cai, T., Luo, S., Zheng, S., Ke, G., He, D., Shen, Y., and Liu, T.-Y. Do transformers really perform badly for graph representation? In *Proceedings of the 35th Conference on Neural Information Processing Systems*, pp. 28877–28888, 2021.

Zha, H., Chen, Z., and Yan, X. Inductive relation prediction by BERT. In *Proceedings of the 36th AAAI Conference on Artificial Intelligence*, pp. 5923–5931, 2022.

Zhang, Y. and Yao, Q. Knowledge graph reasoning with relational digraph. In *Proceedings of the ACM Web Conference 2022*, pp. 912–924, 2022.

Zhu, Z., Zhang, Z., Xhonneux, L.-P., and Tang, J. Neural Bellman-Ford networks: A general graph neural network framework for link prediction. In *Proceedings of the 35th Conference on Neural Information Processing System*, pp. 29476–29490, 2021.

A. Generating Datasets for Inductive Knowledge Graph Completion

Algorithm 2 Generating Datasets for Inductive Knowledge Graph Completion

Input: $\tilde{G} = (\mathcal{V}, \mathcal{R}, \mathcal{E})$, n_{tr} , n_{inf} , p_{rel} , p_{tri}

Output: $\tilde{G}_{\text{tr}} = (\mathcal{V}_{\text{tr}}, \mathcal{R}_{\text{tr}}, \mathcal{E}_{\text{tr}})$ and $\tilde{G}_{\text{inf}} = (\mathcal{V}_{\text{inf}}, \mathcal{R}_{\text{inf}}, \mathcal{E}_{\text{inf}})$

- 1: $\tilde{G} \leftarrow$ Giant connected component of \tilde{G} .
- 2: Randomly split \mathcal{R} into \mathcal{R}_{tr} and \mathcal{R}_{inf} such that $|\mathcal{R}_{\text{tr}}| : |\mathcal{R}_{\text{inf}}| = (1 - p_{\text{rel}}) : p_{\text{rel}}$.
- 3: Uniformly sample n_{tr} entities from \mathcal{V} and form \mathcal{V}_{tr} by taking the sampled entities and their two-hop neighbors. We select at most 50 neighbors per entity for each hop to prevent exponential growth.
- 4: $\mathcal{E}_{\text{tr}} := \{(v_i, r, v_j) | v_i \in \mathcal{V}_{\text{tr}}, v_j \in \mathcal{V}_{\text{tr}}, r \in \mathcal{R}_{\text{tr}}, (v_i, r, v_j) \in \mathcal{E}\}$.
- 5: $\mathcal{E}_{\text{tr}} \leftarrow$ Triplets in the giant connected component of \mathcal{E}_{tr} .
- 6: $\mathcal{V}_{\text{tr}} \leftarrow$ Entities involved in \mathcal{E}_{tr} .
- 7: $\mathcal{R}_{\text{tr}} \leftarrow$ Relations involved in \mathcal{E}_{tr} .
- 8: Let \tilde{G}' be the subgraph of \tilde{G} where the entities in \mathcal{V}_{tr} are removed.
- 9: In \tilde{G}' , uniformly sample n_{inf} entities and form \mathcal{V}_{inf} by taking the sampled entities and their two-hop neighbors. We select at most 50 neighbors per entity for each hop to prevent exponential growth.
- 10: $\mathcal{E}_{\text{inf}} := \mathcal{X} \cup \mathcal{Y}$ such that $|\mathcal{X}| : |\mathcal{Y}| = (1 - p_{\text{tri}}) : p_{\text{tri}}$ where $\mathcal{X} := \{(v_i, r, v_j) | v_i \in \mathcal{V}_{\text{inf}}, v_j \in \mathcal{V}_{\text{inf}}, r \in \mathcal{R}_{\text{tr}}, (v_i, r, v_j) \in \mathcal{E}\}$ and $\mathcal{Y} := \{(v_i, r, v_j) | v_i \in \mathcal{V}_{\text{inf}}, v_j \in \mathcal{V}_{\text{inf}}, r \in \mathcal{R}_{\text{inf}}, (v_i, r, v_j) \in \mathcal{E}\}$.
- 11: $\mathcal{E}_{\text{inf}} \leftarrow$ Triplets in the giant connected component of \mathcal{E}_{inf} .
- 12: $\mathcal{V}_{\text{inf}} \leftarrow$ Entities involved in \mathcal{E}_{inf} .
- 13: $\mathcal{R}_{\text{inf}} \leftarrow$ Relations involved in \mathcal{E}_{inf} .

Algorithm 2 shows how we generate the datasets used in Section 6. Also, Table 5 and Table 6 show the statistic of the datasets and the hyperparameters used to create the datasets, respectively.

As described in Section 3, \mathcal{E}_{tr} is divided into \mathcal{F}_{tr} and \mathcal{T}_{tr} . How to split and use \mathcal{E}_{tr} is a model-dependent design choice. On the other hand, \mathcal{E}_{inf} is divided into three pairwise disjoint sets, \mathcal{F}_{inf} , \mathcal{T}_{val} , and $\mathcal{T}_{\text{test}}$ with a ratio of 3:1:1. For a fair comparison, these three sets are fixed, and the same sets are provided to each model.

In Section 4, we mentioned that we add reverse relations and triplets. While this addition is essential for GNN-based methods (Vashishth et al., 2020; Zhang & Yao, 2022), we should add the reverse relations and triplets after we split \mathcal{F}_{inf} , \mathcal{T}_{val} , and $\mathcal{T}_{\text{test}}$ to prevent data leakage problems. Similarly, we add the reverse relations and triplets after we split \mathcal{F}_{tr} and \mathcal{T}_{tr} .

B. Details about the Baseline Methods

All experiments were conducted with GeForce RTX 2080 Ti, GeForce RTX 3090 or RTX A6000, depending on the implementations of each method. We modified all the baseline models except RAILD and RMPI so that the models accept new relations since they do not consider new relations at inference time. We used the original implementations provided by the authors of the models with minimal modification (if needed) and used the default setting except for the things described below.

Since the original implementations of NeuralLP and DRUM include entities in \mathcal{V}_{tr} as candidates for a prediction task at inference time, we excluded them from the candidates for a fair comparison. On the other hand, the implementations of BLP and RAILD restrict the candidates to be the entities involved in $\mathcal{T}_{\text{test}}$; so we modified this module to consider all entities in \mathcal{V}_{inf} to be candidates.

BLP and QBLP require pre-trained vectors for entities and RAILD requires pre-trained vectors for both entities and relations, where the pre-trained vectors are produced by feeding text descriptions or names into BERT (Devlin et al., 2019). Among our datasets, NL does not have text descriptions, FB has text descriptions only for entities, and WK has text descriptions for both entities and relations. We provided the pre-trained vectors with BLP, QBLP and RAILD using the available information.

We tuned BLP with learning rate $\in \{0.00001, 0.00002, 0.00005\}$ and L2 regularization coefficient $\in \{0, 0.001, 0.01\}$. QBLP was tuned with learning rate $\in \{0.0001, 0.0005\}$, the number of transformer layers $\in \{2, 3, 4\}$ and the number of GCN layers $\in \{2, 3\}$. For Grail, CoMPILE and SNRI, we set the early stop patience to be 10 validation trials and the number of total epochs to be 10. Following the original setting of RMPI, we used the Schema Enhanced RMPI for NL-25, NL-50, NL-75, and NL-100, and used the Randomly Initialized RMPI for NL-0 and NELL-995-v1. We tuned RED-GNN with weight decay $\in \{0.00001, 0.01\}$, dropout rate $\in \{0, 0.3\}$ and the number of layers $\in \{3, 4\}$. We set the early stop patience to be 10 epochs.

Since the implementation of RAILD does not contain the codes for obtaining node2vec representations of relations, we used the official C++ implementation of node2vec³ to calculate the representations of relations.

The original implementation of CompGCN can only be applied to the transductive setting for both entities and relations. We modified CompGCN so that the model also uses randomly initialized embeddings for new entities appearing at inference time. CompGCN is tuned with the number of GCN layers $\in \{1, 2, 3\}$, learning rate $\in \{0.0001, 0.001\}$ and the number of bases $\in \{-1, 20, 40\}$, where -1 denotes the case where each relation has its own embedding. We tuned NodePiece with the size of relational context $\in \{4, 12\}$ and the margin $\in \{15, 20, 25\}$.

Missing Baselines. We could not include PathCon (Wang et al., 2021) and TACT (Chen et al., 2021) in our experiments since their original source codes were written only for relation prediction but not for link prediction. ConGLR (Lin et al., 2022) and CBGNN (Yan et al., 2022) sample 50 negative candidates for each query, following the experimental setting of GraIL. Unlike GraIL, CoMPILE and SNRI, the original implementations of ConGLR and CBGNN do not provide the code for expanding the candidate set to \mathcal{V}_{inf} , so we could not include them as baseline methods. Since the entity sets of training and inference graphs are disjoint in our setting, we could not include baselines assuming new entities should be attached to known entities, such as MEAN (Hamaguchi et al., 2017) and LAN (Wang et al., 2019). We could not include GraphANGEL (Jin et al., 2022) in our experiments because the results in (Jin et al., 2022) are not reproducible.

C. Hyperparameters of INGRAM

For INGRAM, we performed validation every 200 epochs for a total of 10,000 epochs. We tuned INGRAM with 10 negative samples, $d' \in \{32, 64, 128, 256\}$, $\hat{d}' \in \{128, 256\}$, $L \in \{1, 2, 3\}$, $\hat{L} \in \{2, 3, 4\}$, $K \in \{8, 16\}$, $\hat{K} \in \{8, 16\}$, $\gamma \in \{1.0, 1.5, 2.0, 2.5\}$, $B \in \{1, 5, 10\}$ and the learning rate $\in \{0.0005, 0.001\}$. We observed that the best performance of INGRAM is achieved when $B = 10$, showing the effectiveness of our binning strategy used in (3) described in Section 5.1.

Table 5: Datasets for Inductive Knowledge Graph Completion.

| | NL-100 | | | NL-75 | | | NL-50 | | | NL-25 | | |
|------------------------------|-----------------------------|-----------------|-----------------|-----------------|-----------------|-----------------|-----------------|-----------------|-----------------|-----------------|-----------------|-----------------|
| | $ \mathcal{V} $ | $ \mathcal{R} $ | $ \mathcal{E} $ | $ \mathcal{V} $ | $ \mathcal{R} $ | $ \mathcal{E} $ | $ \mathcal{V} $ | $ \mathcal{R} $ | $ \mathcal{E} $ | $ \mathcal{V} $ | $ \mathcal{R} $ | $ \mathcal{E} $ |
| $\widetilde{G}_{\text{tr}}$ | 1,258 | 55 | 7,832 | 2,607 | 96 | 11,058 | 4,396 | 106 | 17,578 | 4,396 | 106 | 17,578 |
| $\widetilde{G}_{\text{inf}}$ | 1,709 | 53 | 3,964 | 1,578 | 116 | 3,031 | 2,335 | 119 | 4,294 | 2,146 | 120 | 3,717 |
| WK-100 | | | | | | | | | | | | |
| | $ \mathcal{V} $ | $ \mathcal{R} $ | $ \mathcal{E} $ | $ \mathcal{V} $ | $ \mathcal{R} $ | $ \mathcal{E} $ | $ \mathcal{V} $ | $ \mathcal{R} $ | $ \mathcal{E} $ | $ \mathcal{V} $ | $ \mathcal{R} $ | $ \mathcal{E} $ |
| | $\widetilde{G}_{\text{tr}}$ | 9,784 | 67 | 49,875 | 6,853 | 52 | 28,741 | 12,022 | 72 | 82,481 | 12,659 | 47 |
| $\widetilde{G}_{\text{inf}}$ | 12,136 | 37 | 22,479 | 2,722 | 65 | 5,717 | 9,328 | 93 | 16,121 | 3,228 | 74 | 5,652 |
| FB-100 | | | | | | | | | | | | |
| | $ \mathcal{V} $ | $ \mathcal{R} $ | $ \mathcal{E} $ | $ \mathcal{V} $ | $ \mathcal{R} $ | $ \mathcal{E} $ | $ \mathcal{V} $ | $ \mathcal{R} $ | $ \mathcal{E} $ | $ \mathcal{V} $ | $ \mathcal{R} $ | $ \mathcal{E} $ |
| | $\widetilde{G}_{\text{tr}}$ | 4,659 | 134 | 62,809 | 4,659 | 134 | 62,809 | 5,190 | 153 | 85,375 | 5,190 | 163 |
| $\widetilde{G}_{\text{inf}}$ | 2,624 | 77 | 11,645 | 2,792 | 186 | 15,528 | 4,445 | 205 | 19,394 | 4,097 | 216 | 28,579 |

Table 6: Hyperparameters Used to Create the Datasets.

| | NL-100 | NL-75 | NL-50 | NL-25 | NL-0 | WK-100 | WK-75 | WK-50 | WK-25 | FB-100 | FB-75 | FB-50 | FB-25 |
|------------------|--------|-------|-------|-------|------|--------|-------|-------|-------|--------|-------|-------|-------|
| n_{tr} | 15 | 60 | 50 | 50 | 20 | 20 | 20 | 30 | 30 | 10 | 10 | 10 | 10 |
| n_{inf} | 80 | 50 | 80 | 80 | 80 | 250 | 15 | 80 | 50 | 20 | 20 | 50 | 50 |
| p_{rel} | 0.40 | 0.40 | 0.40 | 0.40 | 0.00 | 0.30 | 0.40 | 0.30 | 0.50 | 0.40 | 0.40 | 0.30 | 0.25 |
| p_{tri} | 1.00 | 0.75 | 0.50 | 0.25 | 0.00 | 1.00 | 0.75 | 0.50 | 0.25 | 1.00 | 0.75 | 0.50 | 0.25 |

³<https://github.com/snap-stanford/snap/tree/master/examples/node2vec>